Journal of Sound and Vibration (2002) **249**(4), 649–661
doi:10.1006/jsvi.2001.3858, available online at http://www.idealibrary.com on IDEAL®

EXPERIMENTAL STUDY ON THE VORTEX-INDUCED VIBRATION OF TOWED PIPES

S. HONG AND Y. R. CHOI

Korea Research Institute of Ships & Ocean Engineering, KORDI Yusung-gu P.O. Box 23, *Taejon* 305-600, *Korea*

AND

J.-B. PARK, Y.-K. PARK† AND Y.-H. KIM

Department of Mechanical Engineering, Center for Noise and Vibration Control, Korea Advanced Institute of Science and Technology (*KAIST*), 373-1 *Science Town, Taejon* 305-701, *Korea. E-mail*: *yhkim@mail.kaist.ac.kr*

(*Received* 18 *August* 2001, *and in final form* 23 *February* 2001)

We experimentally attempted to understand the vibration characteristics of a flexible pipe excited by vortex shedding. This has been extensively studied in the previous decades (for example, see Sarpkaya 1979 *Journal of Applied Mechanics* **46**, 241–258; Price *et al.* 1989 *Eighth International Conference on Offshore Mechanics and Arctic Engineering, The Hague-March* 19–23, 447–454; Yoerger *et al.* 1991 *Journal of Offshore Mechanics and Arctic Engineering, Transaction of Engineers* **113**, 117–127; Grosenbaugh *et al.* 1991 *Journal of Offshore Mechanics and Arctic Engineering, Transaction of Engineers* **113**, 199–204; Brika and Laneville 1992 *Journal of Fluid Mechanics* **250**, 481–508; Chakrabarti *et al.* 1993 *Ocean Engineering* **20**, 135–162; Jong 1983 *Ph.D. Dissertation, Department of Ocean Engineering*, M. I. T.; Kim *et al.* 1986 *Journal of Energy Resources Technology, Transactions of American Society of Mechanical Engineers* **108**, 77–83). However, there are still areas that need more study. One of them is the relation between spatial characteristics of a flow-induced vibrating pipe, such as its length, the distribution of wave number, and frequency responses. A non-linear mechanism between the responses of in-line and cross-flow directions is also an area of interest, if the pipe is relatively long so that structural modal density is reasonably high. In order to investigate such areas, two kinds of instrumented pipe were designed. The instrumented pipes, of which the lengths are equally 6 m, are wound with rubber and silicon tape in different ways, having different vortex-shedding conditions. One has uniform cross-section of diameter of 26·7 mm, and the other has equally spaced four sub-sections, which are composed of different diameters of 75·9, 61·1, 45·6 and 26·7 mm. Both pipes are towed in a water tank ($200\,\mathrm{m} \times 16\,\mathrm{m} \times 7\,\mathrm{m}$) so that they experienced different vortex-shedding excitations. Various measures were obtained from the towing experiment, including frequency responses, the time-domain tracing of in-line and cross-flow responses, and Wigner–Ville distributions. The experimental results analyzed by using these measures exhibit several valuable features. One of them is that the natural frequencies and their corresponding strain mode shapes dominate the strain response of the uniform pipe. However for those of non-uniform pipe, the responses are more likely local and many modes participate in it.

†Current address: Division of Mechanical Metrology/Force Group, Korea Research Institute of Standards and Science (KRISS), P.O. Box 102, Yusong, Taejon 305–600, Korea.

0022-460X/02/040649 + 13 $35.00/0

1. INTRODUCTION

Elastic structures in flow are subject to flow-induced vibrations. Flow fluctuations and vortices induced from a flow–structure interaction force the structure to vibrate. Such a vibration due to vortex shedding is called a vortex-induced vibration. Sarpkaya [1] reviewed selective topics related to the vortex-shedding vibration such as vortex shedding from a stationary bluff body, wake-oscillator models, dynamic response measurements and flow-fields model, etc.

There have been experiments to study the nature of vortex-induced vibration. Price *et al.* [2] conducted an experiment on five cylinder riser clusters in steady water cross-flow. They found that, in addition to the vortex shedding, the flexible cylinder was also suffering from fluid-elastic-type instability. Grosenbaugh *et al.* [3, 4] analyzed full-scale experiment data on the dynamics and the flow-induced vibration of a long vertical tow cable. They measured the data in the conditions of steady and unsteady towing, while the surface ship was going through a series of starting, stopping, and backing maneuvers at the U.S. Navy's Atlantic Underwater Test and Evaluation Center (AUTEC). From the experiment, the average drag coefficient was measured from 2·2 to 2·5 with errors of $\pm 0{\cdot}24$. Brika and Laneville [5] executed an experimental investigation of the free vortex-induced vibrations of a long flexible circular cylinder with a low damping ratio. The experiment showed that the cylinder's steady response was hysteretic as the flow speed was varied, and that the hysteresis was a fluid-mechanic phenomenon. Chakrabarti *et al.* [6] performed an experiment to determine the effect of three types of two-dimensional shear current (positive shear, no shear, negative shear) on a submerged horizontal circular cylinder. They found that the drag coefficient was larger in shear flow than that in uniform flow at mid-depth of test basin (250 ft long, 33 ft wide, 18 ft depth).

It is an instrumented cable that is widely used to experiment on the characteristics of vortex-induced vibration [7]. References [7–9] show that the well-known "lock-in" is possible for a long cable. In fact, the modal density of the cable is sufficiently low so that a single-mode lock-in is likely possible. To investigate the effect of structural modal density on the response of a long cable, two experiments were performed [8]. These two experiments showed that excitation bandwidth was very important to understand the vibration characteristics of the long pipe subjected to shear flow. A shear parameter was proposed to properly represent its effect on the response. Those experiments also showed that the response of the long pipe could produce a reverberant field or a direct field, depending on the shear parameter. In other words, there is a position where the response is dominated by the resonant modes of pipe, and a location where its vibration is dictated by the frequency content of the force near the location. It is noteworthy, however, that the experiments used considerably long cable (609 and 2758 m) instrumented with only two accelerometers. The number of accelerometers is so few for such a long cable that there is an area that needs more specific study.

In order to investigate the vortex-shedding vibration more thoroughly, we designed an experiment that tows a pipe in a water tank. This pipe towing experiment is the case where the pipe has a length that produces much lower modal density compared with the previous long-cable experiments. This low modal density makes the lock-in possibility higher. Two types of instrumented pipes were used in the experiment. One of them has a uniform cross-section, and the other has a non-uniform cross-section. Therefore, through the whole pipe length, the uniform pipe was excited by the vortex shedding of same frequency, and the non-uniform pipe experienced the vortex-shedding excitation of different frequencies. In the pipe towing experiment, we measured the bending strain at five stations. The figures of strain describe the spatial strain distribution due to the vortex-shedding excitation. Such different results are expected from the viewpoint of the modal density and the spatial distribution of vortex-shedding frequency. In addition to that, by plotting both in-line strain and cross-flow strain simultaneously, the figure-of-eight of bending strain was also observed.

2. EXPERIMENTS

Two types of instrumented pipes were manufactured to mimic two different cases of the vortex-shedding condition. One is uniform vortex shedding along the cylinder. The other is non-uniform shedding. Figure 1 shows the manufactured shapes of uniform pipe and non-uniform pipe. Two stainless-steel pipes of length 6 m whose outer diameter is 21·7 mm were instrumented with strain gauges at five stations (from #1 to #5 in Figure 1) in the longitudinal direction: 28 strain gauges for the uniform pipe and 26 strain gauges for the non-uniform pipe. From the five stations, 16 strain signals were measured simultaneously; 10 for bending (at all stations), three for torsion and three for tension (at station #1, #3 and #5 in Figure 1). After installing the strain gauges on the outer surface of the pipe, the pipe was wound with a rubber tape to make the surface smooth. In addition to that, for the non-uniform pipe that has non-uniform cross-section, a silicon tape was wound so that each of the four sub-sections has different diameters. The diameter of the uniform pipe is 26·7 mm and the diameters of sub-sections of the non-uniform pipe are 75·9, 61·1, 45·6 and 26·7 mm (Figure 1). The total mass of the uniform pipe is 7·18 kg and that of the non-uniform pipe is 19·6 kg.

Impact tests were conducted on the instrumented pipes both in towing water tank and in air. The cross-flow natural frequencies for the uniform pipe are 3·6, 8·5, 15·1, 23·6 and 35·5 Hz (Table 1), listing from the first in-water natural frequency to the fifth one. For the non-uniform pipe, they are 2·1, 4·9, 8·5, 14·3, and 20·5 Hz (Table 2), from the first one to the fifth one. Figures 2 and 3 show the shapes of bending strain and corresponding natural frequencies of the instrumented pipes respectively. The horizontal abscissa represents five measurement points for the bending strain along the pipe length.

Both uniform and non-uniform pipes were towed in a water tank, which is 200 m long, 16 m wide and 7 m deep. Each pipe was installed on a towing carrier to satisfy the boundary

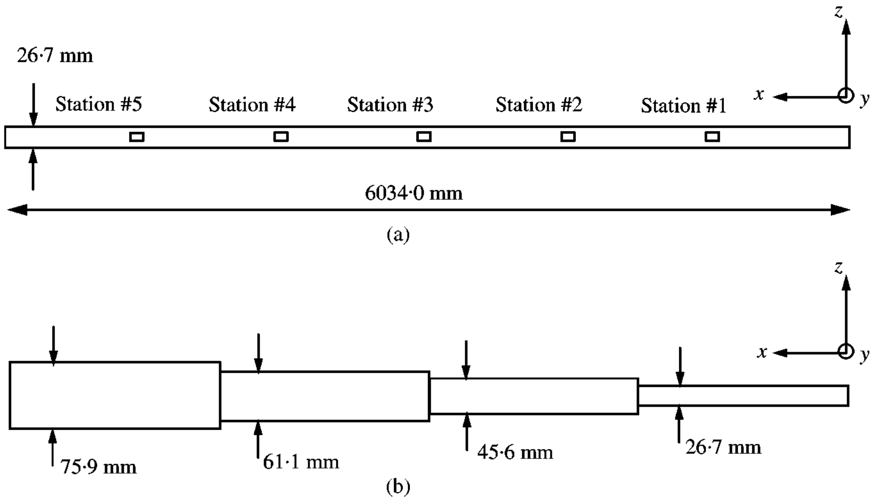

Figure 1. Schematic views of (a) uniform and (b) non-uniform pipes.

TABLE 1

Natural frequencies of the uniform pipe A†

	f_n in air (Hz)			f_n in water (Hz)		
Mode	Analytic	Cross-flow	In-line	Analytic	Cross-flow	In-line
1	4·7	4·6	4·0	3·9	3·6	3·5
2	10·8	9·9	9·9	8·9	8·5	8·8
3	18·9	18·0	17·6	15·6	15·1	15·1
4	29·4	28·4	27·8	24·3	23·6	23·5
5	42·4	40·9	40·8	35·0	35·5	34·4

†Analytic means that the natural frequency in air is obtained by using

$$f_n = \frac{k_1}{2\pi}\sqrt{\left(k_1^2 + \frac{T}{EI}\right)\frac{EI}{m}}, \quad n = 1, 2, 3, 4, 5 \ldots.$$

In water, m is replaced with m_w. $m_w = m + m_a = m + \rho_w \pi (D^2/4)$ where k_1 is the wave number, T is the applied tension, m is the mass per unit length, and ρ_w is the density of water, and the D is the diameter of instrumented pipe.

TABLE 2

Natural frequencies of the non-uniform pipe B

	f_n in air (Hz)			f_n in water (Hz)		
Mode	Analytic	Cross-flow	In-line	Analytic	Cross-flow	In-line
1	N/A†	2·4	2·4	N/A	2·1	2·0
2	N/A	6·0	6·0	N/A	4·9	5·0
3	N/A	10·8	10·9	N/A	8·5	8·7
4	N/A	18·0	18·0	N/A	14·3	14·3
5	N/A	26·0	26·0	N/A	20·5	20·4

†N/A = not available.

conditions of fixed–fixed ends (Figure 4). In addition, by using the winch of carrier, a tension of 1960 N was applied to the instrumented pipe. Figure 4 shows the left half of the combined system of the towing carrier and the instrumented pipe. Two guards of diameter 450 mm were attached at both ends of the pipe so that the flow region around the moving pipe can be considered to be two dimensional. Each pipe was submerged at 600 mm from the free surface, and then towed by the towing carrier at the designed speed. Towing speed is varied from 0·1 to 2·5 m/s with an increment of 0·1 m/s for the uniform pipe. For the non-uniform pipe, the lowest speed was the same as that of the uniform pipe, but the highest speed was 1·8 m/s. We tried to tow the non-uniform pipe at the same speed range as the uniform pipe. However, at the towing speed of 2·0 m/s, the non-uniform pipe was broken at a joint between the carrier and the thickest sub-section of the non-uniform pipe.

From the towing pipe experiments of the uniform and the non-uniform pipe, 16 strain signals of the instrumented pipes were measured simultaneously. Bending strains in the cross-flow and in-line direction were measured at five equally spaced positions along the pipe. Torsion and tension were measured at three positions, station #1, #3 and #5 (Figure 1) as mentioned earlier in this section. The torsion and tension signals were so small

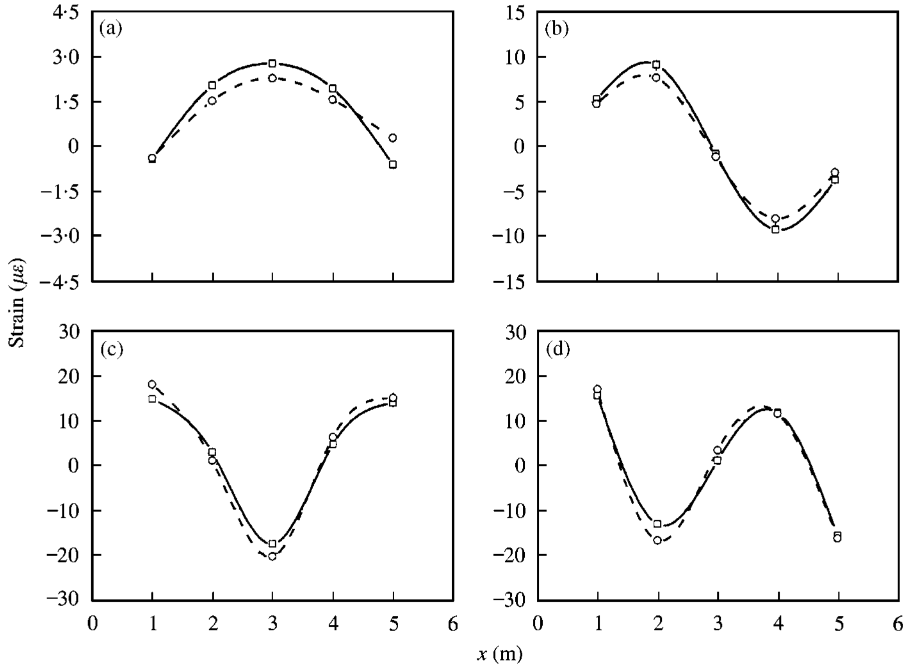

Figure 2. Shapes of bending strain of the uniform pipe in water: (a) first, 3·6 Hz —□—, y direction; – –○– –, z direction; (b) second, 8·5 Hz, —□—, y direction; – –○– –, z direction, (c) third, 15·1 Hz, —□—, y direction; – –○– –, z direction, (d) fourth, 23·6 Hz, —□—, y direction; – –○– –, z direction.

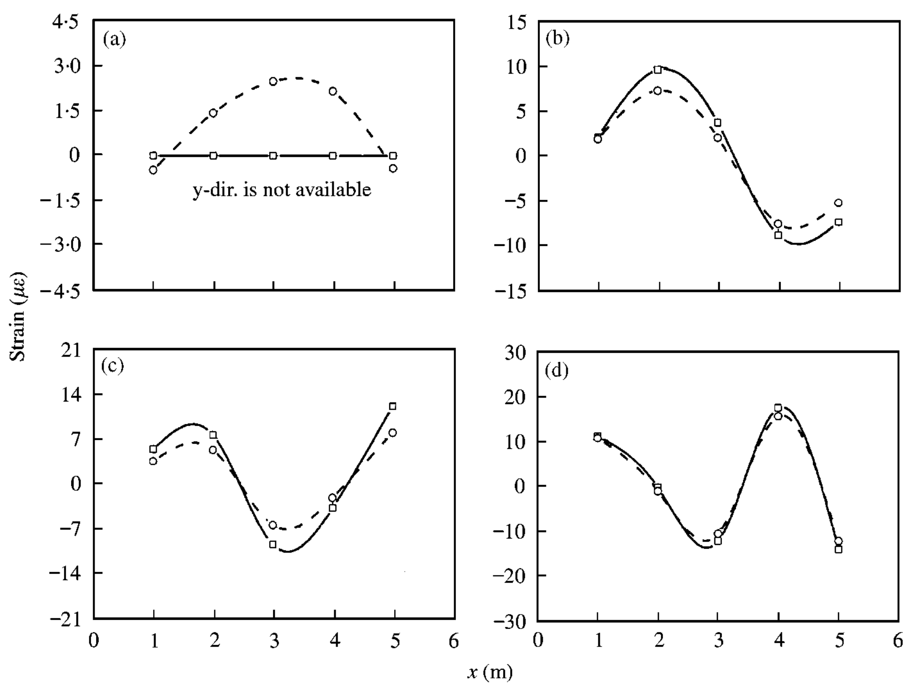

Figure 3. Shapes of bending strain of the non-uniform pipe in water: (a) first, 2·1 Hz, —□—, y direction; – –○– –, z direction; (b) second, 4·9 Hz, —□—, y direction; – –○– –, z direction, (c) third, 8·5 Hz, —□—, y direction; – –○– –, z direction, (d) fourth, 14·3 Hz, —□—, y direction; – –○– –, z direction.

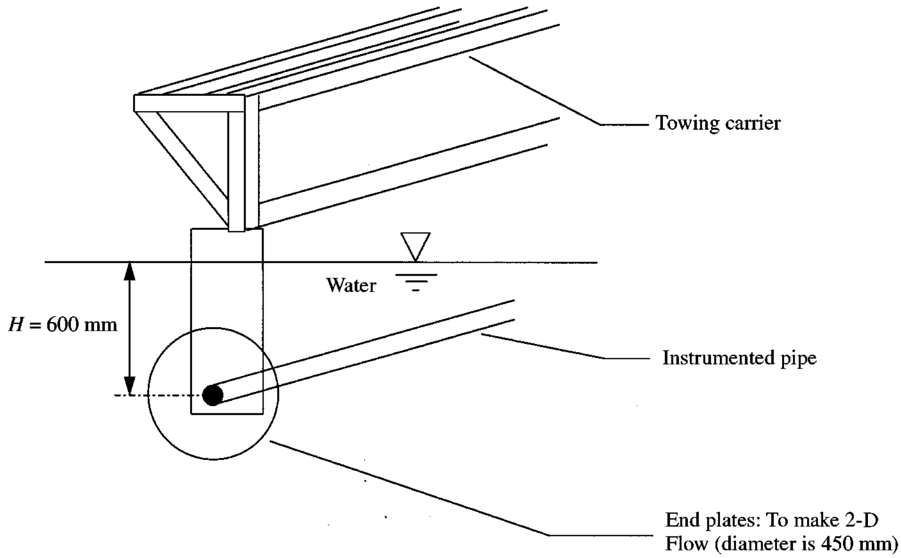

Figure 4. Left-half section of the combined system of a carrier and an instrumented pipe.

in comparison with the bending signal that they were neglected in the analysis process. Sampling frequency was 256 Hz, which allows us to measure the signal up to 128 Hz. The highest shedding frequency for the uniform pipe was expected to be approximately 18·7 Hz, so that the sampling frequency was high enough to avoid aliasing. The record length of data was 48 s, which was determined by considering the maximum towing speed of 2·5 m/s and the travel distance of the carrier. From these strain signals classified by the towing speed, various measures such as strain power spectra, strain variation against the frequency and the towing speed, strain trajectory of in-line and cross-flow directions, and Wigner–Ville distribution were evaluated.

3. EXPERIMENT RESULTS

Towing the uniform and the non-uniform pipes in the water tank, we obtained 16 time signals of strain. From the signals, the power spectra of the pipe strain are obtained. Figures 5, 7, 9, and 10 show the root mean square (r.m.s.) magnitude variation of strain against the frequency and the towing speed.

3.1. UNIFORM PIPE

The uniform pipe towed at the speed range from 0·1 to 2·5 m/s. This range of speed corresponds to the Reynolds number from 2·65E + 03 to 6·63E + 04. In this range of Reynolds number, fully turbulent vortex street is formed in wake [10]. These vortices interact with the instrumented pipe so that its cross-flow vibration is governed by the pressure variation due to the vortex shedding. It means that the vibration of the instrumented pipe is synchronized with the frequency of the vortex shedding. This phenomenon is called “lock-in”. The vortex-shedding frequency can be inferred from the power spectrum of cross-flow vibration of the instrumented pipe.

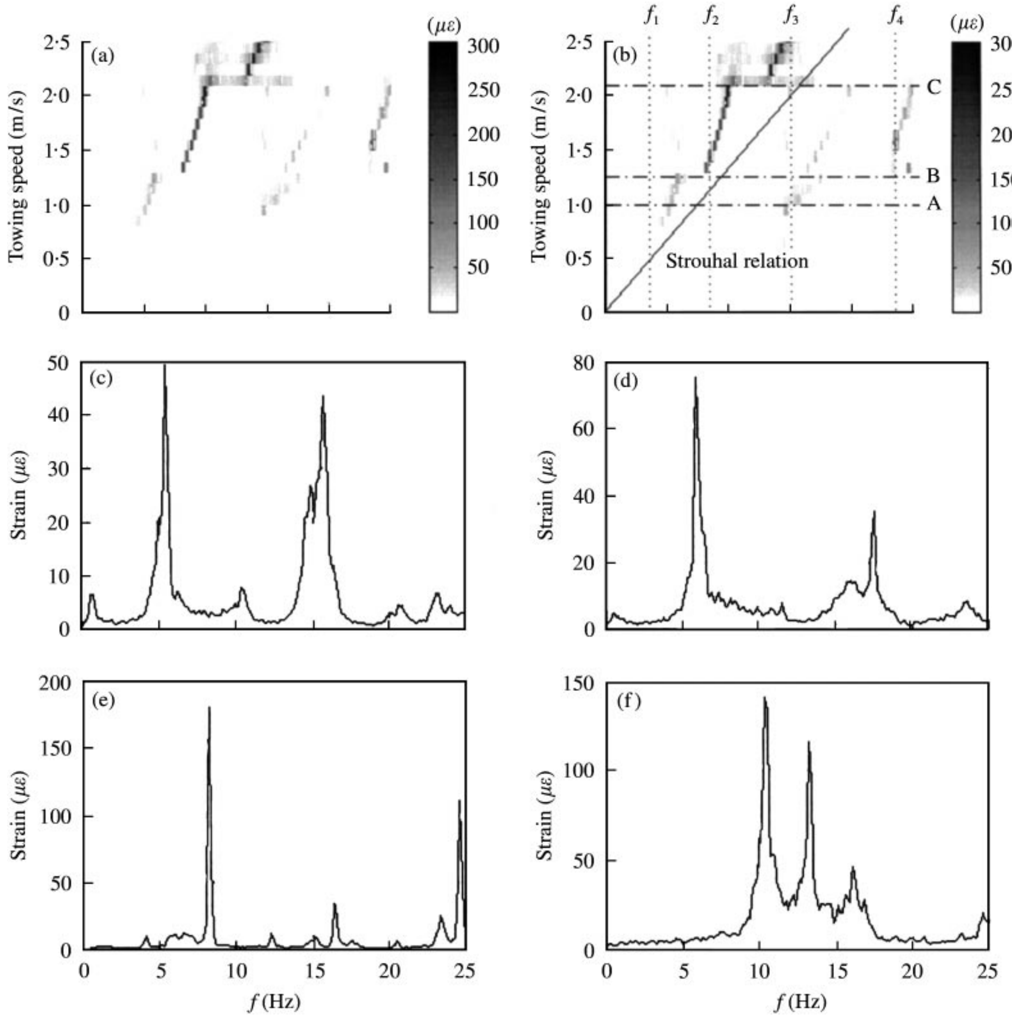

Figure 5. Strain (r.m.s.) response at station #1 of the uniform pipe in the cross-flow direction. (The towing speeds ranges from 0·1 to 2·5 m/s with an increment of 0·1 m/s): (a) station #1, (b) station #1 (A replica of Figure 5(a)), (c) towing speed 1 m/s (line A), (d) towing speed 1·2 m/s (under the line B), (e) towing speed 1·3 m/s (upper the line B), (f) towing speed 2·1 m/s (line C).

Figure 5 is the cross-flow strain response at station #1 of the uniform pipe (Figure 1). The results of the other four stations are like that of station #1. Figure 5(b) is the same as Figure 5(a) except for the several additional lines to make the analysis convenient. The solid line on Figure 5(b) expresses the Strouhal relation. The vertical dot lines on the figure are resonance frequencies in still water that are 3·6, 8·5, 15·1 and 23·6 Hz (Table 1). The horizontal dash–dot lines A, B and C represents the towing speeds 1, 1·25 and 2·1 m/s respectively.

Figure 5(a) demonstrates that the vibration often passes suddenly from one resonance to another depending on the towing speed. Dale, Nenjel and McCandles have measured comparable results from towing flexible cable 3 ft long and 0·1 in in diameter [10]. However, the data of Figure 5 are measured by varying the towing speed. The slowest one is 0·1 m/s. The fastest speed is 2·5 m/s. The increment is 0·1 m/s. Therefore, we have 25 discrete data with respect to the towing speed.

Figure 5 essentially depicts the way in which the shedding frequency and structural natural frequencies interact with each other. As the carrier frequency increases, the shedding frequency also increases. For example, when the carrier tows the structure by 1 m/s (Line A or Figure 5(c)), the dominant frequency of response is about 5 Hz. This peak frequency varies but does not follow the well-known Strouhal relation as shown in Figure 5(b). That is

$$f_s = S_t \frac{V}{D}, \tag{1}$$

where f_s is the shedding frequency, S_t is the Strouhal number, V is the flow speed and D is the diameter of the pipe.

Equation (1) describes the Strouhal relation. One reason for the difference from the Strouhal relation is that the instrumented pipe is not rigid, and the other is due to the lock-in phenomenon. The higher response at resonance broadens the lock-in band so that the vortex shedding occurs near the resonance frequency [11, 12]. Owing to this characteristic, the response near the second resonance frequency of 8·5 Hz has a tougher slope. Such a slope means that the vortex-shedding frequency is synchronized with the higher response near the resonance frequency.

Figures 5(d) and 5(e) show the transition of peak across the line B of Figure 5(b), where the primary response frequency changes to the second natural frequency. At the towing speed of 1·2 m/s, there is no such frequency component of it. However, at the towing speed of 1·3 m/s, there comes the second resonance of 8·5 Hz as primary peak. At the towing speed of 2·1 m/s (line C or Figure 5(f)), we can see that the response frequency changes but it jumps to another resonance frequency at the same speed. However, the two peak frequencies do not coincide exactly with second and third resonances respectively. Since the response, in the vicinity of a resonance, is also relatively high, it causes the lock-in band to be broadened.

The second peaks in a magnitude, in the range from line B to line C, are not the cross-flow strain but the in-line strain. The strain gauges in the cross-flow direction are installed to measure solely the cross-flow bending deformation. However, as can be seen in Figure 6, a strain gauge generates a signal against both the longitudinal tension deformation and the transverse bending deformation. In the vortex-shedding vibration, the combined in-line and cross-flow vibration causes the strain in the both directions which are measured simultaneously.

The in-line strain response at station #1 of the uniform pipe is plotted in Figure 7. Figure 7(b) is the replica of Figure 7(a). The difference between them is only the two lines (D1 and D2). The in-line response shows that the in-line strain signal is seriously contaminated by the transverse bending deformation of the strain gauge. However, in the order of magnitude sense, the well-known frequency doubling in the in-line response is quite obvious. For

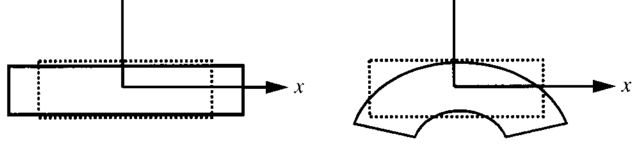

Figure 6. (a) Longitudinal tension deformation and (b) transverse bending deformation of strain gauge: ⋯, original shape; ☐, deformed shape.

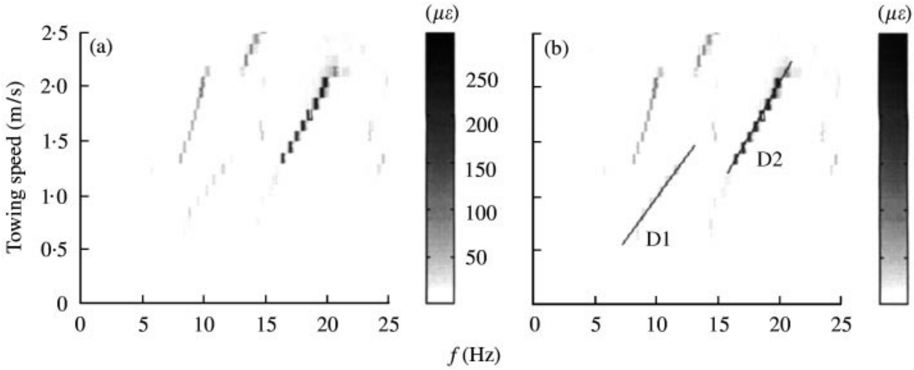

Figure 7. Strain (r.m.s.) response at station #1 of the uniform pipe in the in-line direction (the towing speeds ranges from 0·1 to 2·5 m/s with an increment of 0·1 m/s): (a) station #1, (b) station #1 (a replica of Figure 6(a)).

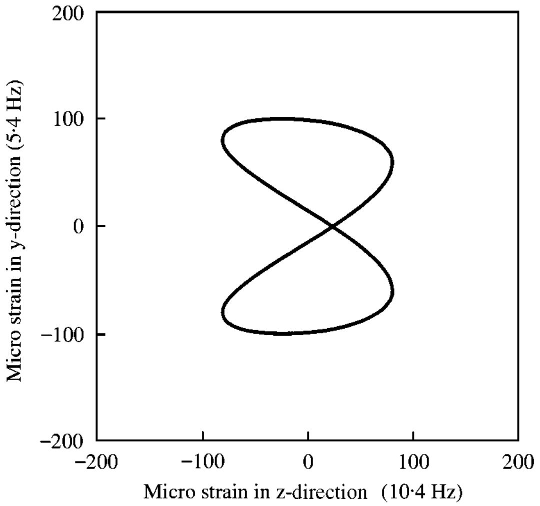

Figure 8. Y–Z plane trajectory of micro stains when the uniform pipe is towed at 1·0 m/s. Two dominant modes in the y and z directions show the "8" shape.

example, see the primary frequency when the towing speed is 1·5 m/s in Figures 5(b) and 7(b). Figure 8 shows the way in which the structure vibrates in the cross-flow and the in-line direction.

3.2. NON-UNIFORM PIPE

The non-uniform pipe was towed at the speed range from 0·1 to 1·8 m/s. This speed range corresponds to the Reynolds number from 2·65E + 03 to 1·36E + 05. In this range of Reynolds number, fully turbulent vortex street is formed in wake [10]. The cross-flow strain response at station #1 of the non-uniform pipe is shown in Figure 9. The results of the other four stations are similar to that of station #1. Both Figures 9(a) and 9(b) are the same except that Figure 9(b) has four lines that show the Strouhal relation of each of the four sub-sections. The thicker the diameter is, the steeper the Strouhal relation expressed in the

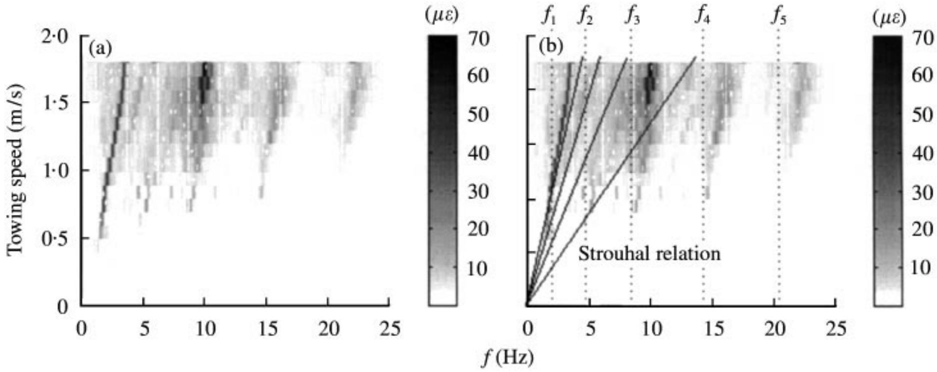

Figure 9. Strain (r.m.s.) response at the station #1 of the non-uniform pipe in the cross-flow direction (the towing speeds ranges from 0·1 m/s slowest to 1·8 m/s fastest with an increment of 0·1 m/s): (a) station #1, (b) station #1 (a replica of Figure 9(a)).

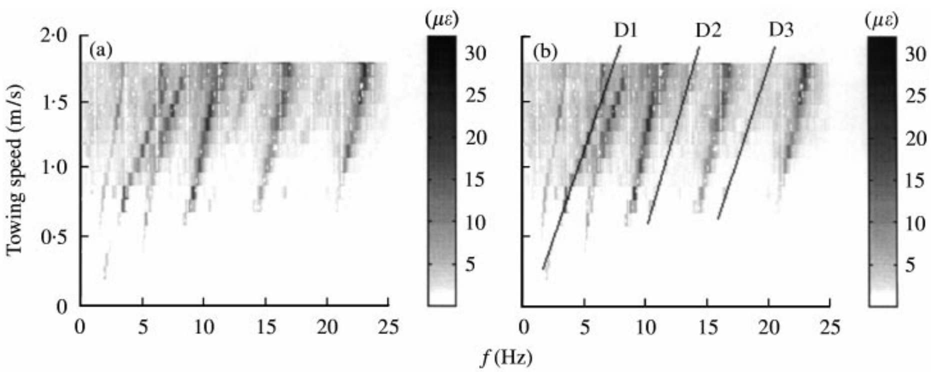

Figure 10. Strain (r.m.s.) response at the station #1 of the non-uniform pipe in the in-line direction (the towing speeds ranges from 0·1 m/s slowest to 1·8 m/s fastest with an increment of 0·1 m/s): (a) station #1, (b) station #1 (a replica of Figure 10(a)).

figure is. Those dot lines represent the resonance frequencies such as 2·1, 4·9, 8·5, 14·3 and 20·5 Hz (Table 1).

As a consequence of the non-uniform cross-section, the shedding frequencies of each of the four sub-sections are different. In other words the non-uniform pipe is excited by vortices at four different shedding frequencies. The fundamental resonance governs the vibration in the speed range from 0·1 to 2·5 m/s. This means that the excitation of the thickest part dominates the entire vibration of the pipe.

The strain response at station #1 of the non-uniform pipe in the in-line direction is given in Figure 10. Figure 10(b) is a copy of Figure 10(a). In Figure 10(b), the three lines (D1–D3) represent the doubled frequencies of cross-flow vibration. Although there must be only the doubled frequencies of the cross-flow vibration, both the components are observed simultaneously. As we see the in-line response of the uniform pipe, this is also due to the transverse bending deformation of the strain gauge. It is noteworthy that the magnitude of the in-line response is very small compared with that of cross-flow.

The highlight of these experimental results, both cross-flow and in-line ones, is that all the frequency components are involved in the response. There is no frequency jump that we

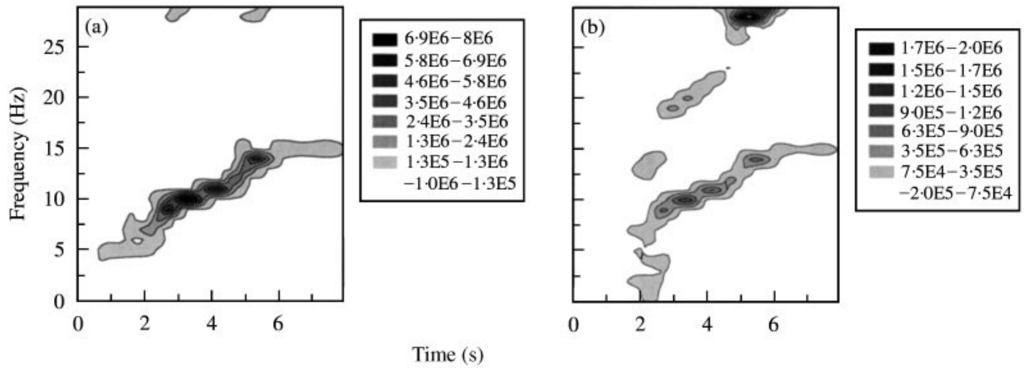

Figure 11. Wigner–Ville distributions of the strain responses of the uniform pipe A at #4 when it is towed by increasing the speed from 0·1 to 2·5 m/s. (a) Cross-flow direction: (b) In-line direction.

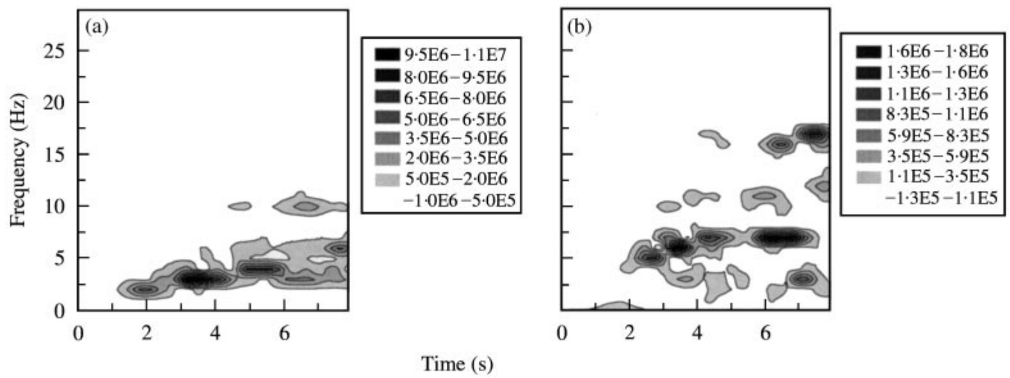

Figure 12. Wigner–Ville distributions of the strain responses of the non-uniform pipe B at #4 when it is towed by increasing the speed from 0·1 to 1·8 m/s. (a) Cross-flow direction: (b) In-line direction.

observed in the case of the uniform pipe. Therefore the lock-in is not likely possible for the non-uniform case.

3.3. WIGNER–VILLE DISTRIBUTION

Figure 11 shows the Wigner–Ville distribution of the uniform pipe measured at station #4, when the pipe was towed at the speed range from 0·1 to 2·5 m/s. The towing speed was linearly increased. Thus, the shedding excitation frequency changed continually from 0·8 to 18·7 Hz. The response of the cross-flow direction clearly shows the lock-in phenomenon. The dominant frequencies do not change linearly with the towing speed. The dominant frequency stays for a while, then transits to the next frequency. This same result of the different analysis again confirms what we observed in Figure 5. The in-line responses show typical frequency doubling characteristics; there are also the responses of the same frequency of the cross-flow direction, but this is just because the measurement system does not perfectly separate the deformation in the direction of cross-flow from that of in-line. Figure 12 depicts the Wigner–Ville distribution of the non-uniform cylinder when it was towed with changing speed from 0·1 to 1·8 m/s. It is obvious that the bandwidth is much wider than that of the uniform case (Figure 11). It is also seen that the low-frequency response is dominant, independent of the towing speed. As discussed earlier, the low-frequency response is due to the vortex shedding of the largest section of the pipe.

4. CONCLUSIONS

Experimental study on vortex-induced vibration of pipes with circular cross-section was performed in the towing water tank. The towing water tank provided a fairly controllable experiment condition. Two steel pipes were instrumented by strain gauges and were prepared in two types: one of uniform cross-section and the other of non-uniform cross-section.

It was found that there are distinct differences between the responses of the uniform and the non-uniform pipes. The responses of the uniform pipe are dominated by single frequency and a famous frequency jump was observed. On the other hand, the responses of the non-uniform pipe are more likely governed by many frequency components. For the case of the non-uniform pipe, the low-frequency vortex shedding is induced from the large cross-section, and the high-frequency vortex shedding is generated from the smaller section. The low-frequency response induced from the largest section of pipe dominates the entire response of the non-uniform pipe. These multiple phenomena of vortex shedding with different frequencies make the excitation range of the non-uniform pipe broader than that of the uniform pipe. Wigner–Ville distributions clearly show such a different excitation range.

These experimental results reveal an aspect of the characteristic differences of vortex-shedding vibrations of a pipe in uniform flow and in shear flow. The towing conditions of the uniform pipe in a water tank are equivalent to those of the uniform flows to the pipe. The characteristic phenomena of the vortex shedding of the non-uniform pipe could be interpreted as a simulated vortex-shedding condition around the uniform pipe in the corresponding shear flow.

ACKNOWLEDGMENT

The authors acknowledge that this experimental study was performed as a research topic initiated by the *Ministry of Science and Technology of Korea* and appreciate their full support throughout the research work.

REFERENCES

1. T. SARPKAYA 1979 *American Society of Mechanical Engineers Journal of Applied Mechanics* **46**, 241–258. Vortex-induced oscillations, a selective review.
2. S. J. PRICE, M. P. PAIDOUSSIS, B. MARK and W. N. MUREITHI 1989 *Eighth International Conference on Offshore Mechanics and Arctic Engineering. The Hague-March* 19–23, 447–454. Current-induced oscillations and instabilities of a multi-tube flexible riser: water tunnel experiments.
3. D. R. YOERGER, M. A. GROSENBAUGH, M. S. TRIANTAFYLLOU and J. J. BURGESS 1991 *Journal of Offshore Mechanics and Arctic Engineering, Transactions of American Society of Mechanical Engineers* **113**, 117–127. Drag forces and flow-induced vibrations of a long vertical tow cable. Part I: steady-state towing conditions.
4. M. A. GROSENBAUGH, D. R. YOERGER, F. S. HOVER, M. S. TRIANTAFYLLOU and J. J. BURGESS 1991 *Journal of Offshore Mechanics and Arctic Engineering, Transactions of American Society of Mechanical Engineers* **113**, 199–204. Drag forces and flow-induced vibrations of a long vertical tow cable. Part II: unsteady towing conditions.
5. D. BRIKA and A. LANEVILLE 1992 *Journal of Fluid Mechanics* **250**, 481–508. Vortex-induced vibrations of a long flexible circular cylinder.

6. S. K. Chakrabarti, D. C. Cotter and P. Palo 1993 *Ocean Engineering* **20**, 135–162. Shear current forces on a submerged cylinder.
7. J. Jong 1983 *Ph.D. Dissertation, Department of Ocean Engineering, M.I.T.* The quadratic correlation between in-line and cross-flow vortex-induced vibration of long flexible cylinders.
8. Y.-H. Kim, J. K. Vandiver and R. Holler 1986 *Journal of Energy Resources Technology, Transactions of American Society of Mechanical Engineers* **108**, 77–83. Vortex-induced vibration and drag coefficients of long cables subjected to sheared flow.
9. J. K. Vandiver and T. Y. Chung 1988 *American Society of Mechanical Engineers Winter Annual Meeting, Symposium on Vortex-Induced Vibration, Chicago*. Predicted and measured response of flexible cylinders in sheared flow.
10. R. D. Blevins 1990 *Flow-Induced Vibration*, 43–102. New York: Van Nostrand Reinhold; second edition.
11. G. H. Koopmann 1967 *Journal of Fluid Mechanics* Part 3, **28**, 501–512. The vortex wake of vibrating cylinders at low Reynolds numbers.
12. P. K. Stansby 1976 *Journal of Fluid Mechanics* Part 4, **74**, 641–665. The locking-on of vortex shedding due to the cross-stream vibration of circular cylinders in uniform and shear flows.